Angle-dependent spin crossover properties in polymorphic iron(ii) complexes based on pyridine-triazole derivatives

Emmelyne Cuza, Nicolas Delsuc, Jerôme Marrot, William Shepard, Clotilde Policar, Christian Serre, Antoine Tissot

Angle dependance Spin Crossover properties in polymorphic Iron(II) complexes based on pyridine-triazole derivatives

Emmelyne Cuza,*[a] Nicolas Delsuc, [b] Jerôme Marrot,[c] William Shepard,[d] Clotilde Policar,[b] Christian Serre[a], Antoine Tissot*[a]

Two new Fe(II) compounds based on a pyridine-triazole ligand with NCS^- co-ligand were synthesized as thermodynamic **(1)** and kinetic **(2)** products. Single crystal X-Ray diffraction evidenced that these compounds are polymorphs. Magnetic susceptibility of each compound was recorded and showed that **(1)** undergoes a sharp spin crossover, while **(2)** remains high spin across the temperature range. We discussed here the importance and the impact of the crystalline packing on the switching properties of these compounds.

Introduction

In the switchable materials field, the design of new coordination compounds exhibiting spin crossover (SCO) behavior, i.e. the ability to switch their spin state from high-spin (HS) to low-spin (LS), is a challenge.[1] Such conversion is possible via external stimuli such as temperature, pressure, magnetic field or light irradiation, as well as chemical perturbation,[1-2] and occurs principally in the first row of transition metals with d^4 to d^7 electronic configurations. Fe(II) SCO complexes, which can go from a paramagnetic HS (S=2) to a diamagnetic LS state (S=0) states, are by far the most studied.

In order to design coordination compounds with iron(II), a large panel of ligands have already been explored, mainly based on N-donor atoms (Figure.1).[3-16] For example in the case of the tzpy (3-(2-pyridyl)-[1,2,3]triazolo[1,5-a]pyridine)[4-7] ligand, thermal spin crossover has been observed when associated with a NCX^- anion as ligand for charge balancing, leading to the neutral compound $[Fe(tzpy)_2(NCX)_2]$ (X = S or Se) that presents a ligand field strength compatible with a thermal spin state switching. However, surprisingly, bidentate ligands combining a pyridine and a simple triazole ring have not been used to the same extent to design spin crossover compounds compared to the abpt (abpt = 4-amino-3,5-bis(pyridin-2-yl)-1,2,4-triazole) ligand type (Figure.1).

Around 16 mononuclear Fe(II) complexes structures have been reported with (2-pyridyl)-1*H*-1,2,3-triazol-1-R linkers including tzpy ones,[5-12] and 11 polynuclear Fe(II) compounds.[11-16] On all of these, only 10 have had their magnetic properties discussed and 6 of them show SCO properties. For mononuclear Fe(II) compounds with other groups than tzpy, only 2 show SCO properties[5]: $[Fe(FTP)_2(NCX)_2]\cdot CHCl_3$ with (X = S or Se) respectively showing an incomplete thermal transition for $[Fe(Fc\text{-}tzpy)_2(NCS)_2]\cdot CHCl_3$ ($T_{½}$ = 85 K with T_{LIESST} of 47 K) and a quantitative conversion for $[Fe(FTP)_2(NCSe)_2]\cdot CHCl_3$ ($T_{½}$ = 168 K and a T_{LIESST}= 39 K). On the opposite, the other compounds were stuck in HS or LS states at any temperature.[6-7, 11-12]

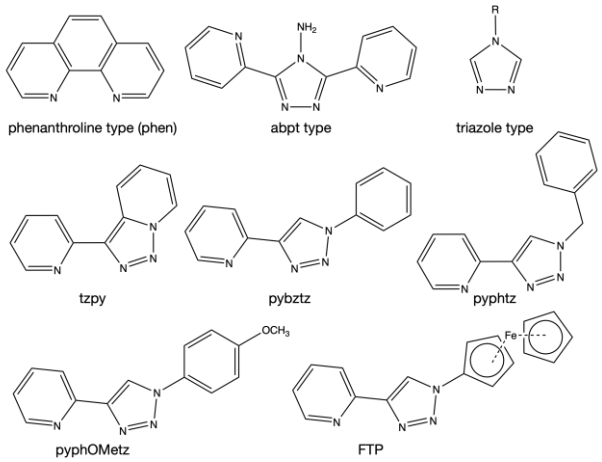

Figure.1 Examples of N-donor common ligands used to build Fe(II) SCO compounds, and bidentate ligand based on 1,2,3-triazole.

The use of 1,2,3-triazole rings have been a key point for developing new ligands.[4] In the past, 1,2,4-triazole rings and derivatives ligands have been mostly used, and led to a wide range of SCO compounds, such as monuclear[17], trinuclear complexes [19-20] as well as coordination polymers.[17] Thus, considering the interesting SCO properties of some of these compounds including abrupt transition close to room temperature, photoswitching, etc. we decided to look into the design of a functional pyridine-1,2,3-triazole ligand previously developed by some of us for applications in imaging.[18-21] In this study, a O-Methyl group was added on the ligand to enhance the probability of getting weak intermolecular interactions between mononuclear complexes, which may have a huge impact on the switching properties and possibly induce cooperative transitions.

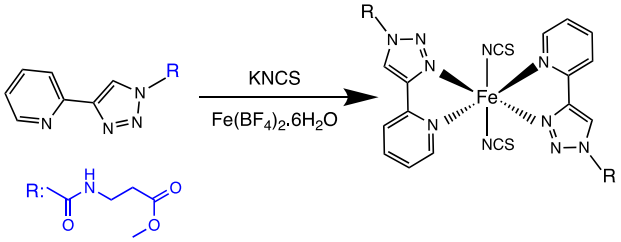

Scheme.1 Synthesis scheme of $[Fe(PytaCOOMe)_2(NCS)_2]$ complexes.

We report here the synthesis and characterization of $[FeL_2(NCS)_2]$ (L = PytaCOOMe) (Scheme.1), a new Fe(II) complex that

crystallizes in the form of two polymorphs noted **(1)** and **(2)**. The different synthetic conditions used to prepare each compound vary substantially, allowing us to identify that **(2)** is the kinetic product and **(1)** the thermodynamic one. Polymorphism arises from a difference in conformation/arrangements of the molecules in the packing/unit-cells when crystallization occurs. Even though they are chemically identical, their physical properties can be highly impacted. Polymorphism is not that common in SCO compounds and when polymorphism is observed, the SCO behavior can be severely altered. [22-28] Since the first SCO polymorphs were discovered,[22] the subject has been studied over the years and enabled a better understanding on the link between packing and SCO behavior.[28-29] However, the number of polymorphs presenting huge difference in SCO properties are still limited, and are yet to be explored thoroughly. Here, **(1)** and **(2)** present a huge difference in their magnetic properties, with **(1)** undergoing a sharp thermal spin-crossover upon cooling contrary to **(2)** that stays in HS state down to 10 K. These differences are discussed to evidence the key structural factor at their origin.

Results and discussion

Synthetic procedures

The compound PytaCOOMe (L) was prepared according to the previously published procedure [30] (See Experimental). The complex $[FeL_2(NCS)_2]$ was prepared by slow diffusion in fine glass tube as yellow single-crystals **(1)** and was obtained by fast evaporation of a methanol/water solution of the complex **(2)**. The infrared spectra are identical as the two compounds are polymorphs (slight shifting due to equipment precision), with a strong absorption band at 2049 cm^{-1} for **(1)** and **(2)**, which can be assigned to the asymmetric stretching vibration modes ($\nu_{(C\equiv N)}$) of the thiocyanato group coordinated to a HS Fe(II) cation (see Figures.S1, S3 and S5). Some particular vibrations can be pointed to such as bands at 3331 and 1665 cm^{-1} corresponding to the amide group, a band at 1733 cm^{-1} corresponding to the ester group and bands at 1610-920 cm^{-1} corresponding to the aromatic rings.

Magnetic measurements

The magnetic measurements were recorded on polycrystalline samples for which powder X-ray diffraction patterns were recorded to ensure the high purity of the compounds (See Figure.S2 and S4). Figure.2 presents the variable temperature magnetic susceptibility measured between 50 and 300 K for **(1)** and between 10 and 300 K for **(2)**. Both compounds are HS at 300 K, with corresponding χ_mT products of 3.38 cm^3 K mol^{-1} for **(1)** and 3.37 cm^3 K mol^{-1} for **(2)**, as expected for an isolated Fe(II) ion. Upon cooling, the χ_mT value of **(1)** remains constant until 200 K and then undergoes an abrupt transition centered around $T_{½}$ = 150 K that is perfectly reversible upon warming. At 50 K, a χ_mT of 0.09 cm^3 K mol^{-1} is obtained, indicating that the compound is almost fully LS.

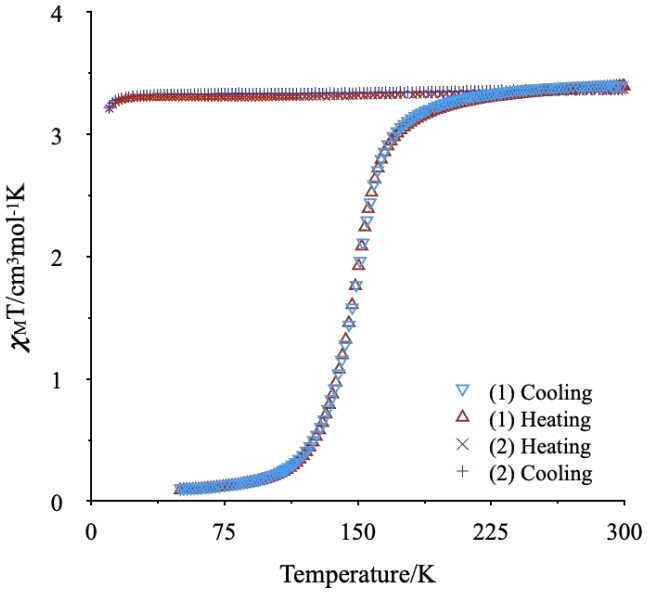

*Figure.2 Evolution of the product of the molar magnetic susceptibility by the temperature as function of the temperature ($(\chi_mT)vs(T)$) for compounds **(1)** and **(2)**.*

In comparison, compound **(2)** remains HS throughout the temperature range explored, with only a slight decrease of the χ_mT product below 20 K than can be attributed to the zero field splitting (ZFS) of the HS Fe(II) ions.

Structural analysis of (1) and (2)

The crystal structure of both compounds was determined at 110 K and 200 K for **(1)** and at 180 K for **(2)**. For **(1)**, the data were recorded using a microfocused synchrotron beam (PROXIMA2 at SOLEIL Synchrotron) due to the small size of the crystal. The unit cell parameters, crystal refinement data, and the pertinent bond distances and angles of both structures are summarized in Table.1 and 2.

Compound	(1)	(1)	(2)
Temperature / K	110	200	180
Color	red	yellow	Yellow
Formulae	$C_{28}H_{30}FeN_{12}O_6S_2$	$C_{28}H_{30}FeN_{12}O_6S_2$	$C_{28}H_{30}FeN_{12}O_6S_2$
Space group	$P2_1/c$	$P2_1/c$	$P2_1/c$
System	Monoclinic	Monoclinic	Monoclinic
a /Å	13.4990(3)	13.5277(8)	13.271(3)
b /Å	14.2794(4)	14.6210(7)	13.139(3)
c /Å	9.1679(3)	9.2130(6)	9.619(2)
β / °	103.635(3)	103.732(5)	99.910(7)
V / Å³	1717.38(11)	1770.14(18)	1652.3(6)
Z	2	2	2
Tot reflexion	17135	16974	31560
Unique reflexion / R_{int}	3006/0.0652	2920/0.1076	2930/0.1771
GooF[c] sur F^2	1.015	0.862	1.170
R_1[a] on $I > 2\sigma(I)$ / wR_2[b] (all)	0.0714/ 0.2356	0.0740/0.2036	0.0937/0.1812

[a] $R_1 = \Sigma|Fo\text{-}Fc|/Fo)$; [b] $wR_2 = [\Sigma((\omega(Fo^2\text{-}Fc^2))^2/(\omega Fo^2)^2)]^{1/2}$; [c] $GooF = [(\Sigma(\omega(Fo^2\text{-}Fc^2))^2/(N_{obs}\text{-}N_{var})]^{1/2}$.

*Table.1 Crystal data and structure refinement of the compounds **(1)** and **(2)**.*

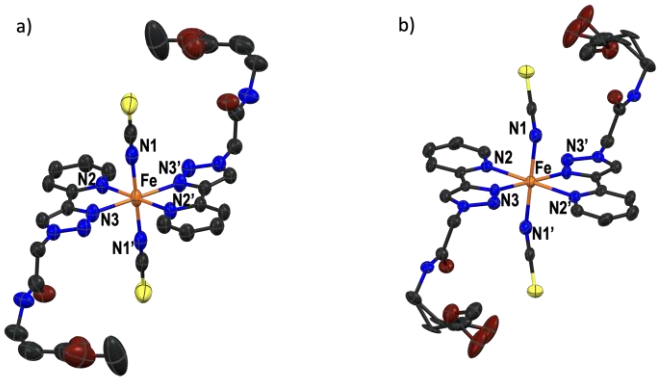

*Figure.3 Representation of asymmetric unit of the complex a) in **(1)** at 200 K and b) in **(2)** at 180 K.*

Compounds **(1)** and **(2)** crystallize in the $P2_1/c$ monoclinic space group, which was confirmed using powder X-ray diffraction (PXRD). PXRD also show unambiguously that both compounds are different, confirming that they are polymorphs (Figure.S6), even though their lattice are similar. Both asymmetric units are composed of $Fe(PytaCOOMe)_2(NCS)_2]$ centred on a crystallographic inversion centre (localized on the Fe centre). Both compounds are composed of two bidentate ligand PytaCOOMe and two thiocyanate ligands coordinated in a μ-NCS fashion in axial position. Such arrangement led to the general crystallographic formula of two $[Fe(PytaCOOMe)_2(NCS)_2]$ complexes per unit-cell (Figure.3).
The Fe(II) ions are hexa-coordinated by six nitrogen atoms giving a distorted FeN_6 octahedron, coming from terminal thiocyanato ligands nitrogen atoms (N1 and N1') and from nitrogen atoms (N2, N2', N3, N3') of the two PytaCOOMe chelating ligands.

Close examination of the average Fe-N bond distances and N-Fe-N angle and distortion parameter (Table.2) give in-dept information about the metal environment around the distorted octahedra in both compounds. For compound (**1**) at 110 K, the average $<d_{Fe1-N}>$ = 2.0165 Å and the values of distortion parameters of Σ = 52.29° and Θ = 201.20° demonstrate that the compound is in the LS state. On the contrary at 200 K, the same compound (**1**) shows higher deformation of the octahedron, with $<d_{Fe1-N}>$ = 2.1489 Å and of Σ = 67.41° and Θ = 262.01°, value which are similar to those found for compound (**2**) ($<d_{Fe1-N}>$ = 2.1489 Å, Σ = 70.86° and Θ = 260.06°), indicating that both complexes are in the HS state. To understand the difference in the magnetic properties between both compounds, their structures were carefully compared, starting with a full description of compound (**1**) in HS and LS state.

Bond lengths (Å)	**(1)**-110 K	**(1)**-200 K	**(2)**
d<Fe-N> (Å)	2.0165	2.1480	2.1720
Angle <N-Fe-N>			
Σ <N-Fe-N>	52.29	67.41	70.86
Θ <N-Fe-N>	201.20	262.01	260.06

*Table.2: Crystal data and structure refinements of the compounds **(1)** and **(2)**.(Σ & Θ)[31]*

Comparison of the compound (**1**) in HS and LS state is depicted in Figure.4. The overlaid structures shows that the structures are similar and the main difference arises from the deformation of the octahedron (Table S.23), principally due to the N2-Fe1-N3 angle which tend to get closer to 90° at LT.

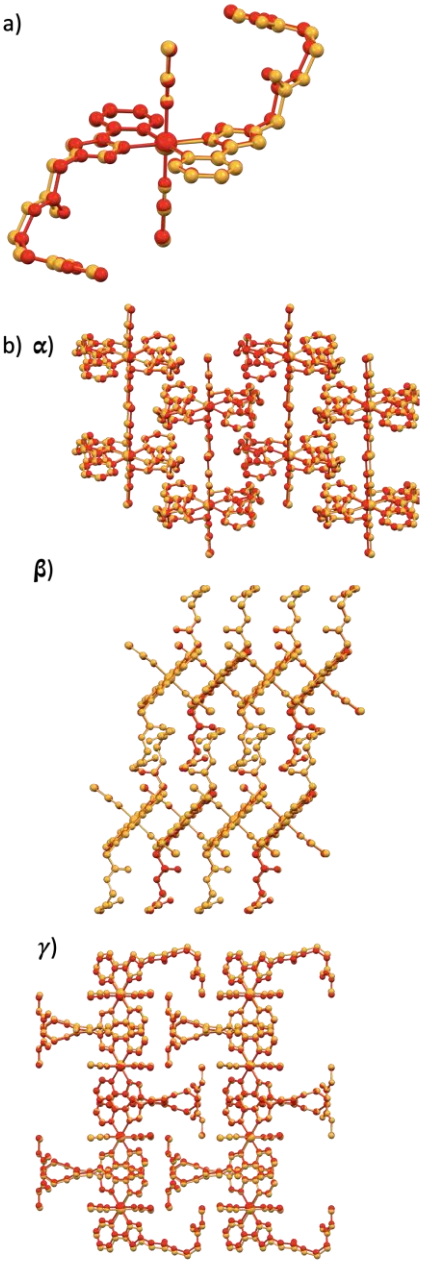

*Figure.4 a) Overlay of compound **(1)** at 110K in red and **(1)** at 200 K in orange. b) Packing representation of **(1)** at 110 K and 200 K in the 011 plane (**α**), in the 101 plane (**β**) and in the 110 plane (γ)*

By analyzing the packing, similarities can be found between polymorphs **(1)** and **(2)**. The ac plane (101) and ab plane (110) are quite similar in both structures (See Figure.S7), with the ac planes being equivalent by a rotation of 180° on [001] axis and the ab planes equivalents by a rotation of 180° on the [010] axis (Figure.S8). For the bc plane (011) no translation or rotation can lead to any equivalence between the structure, as seen in Figure.5.

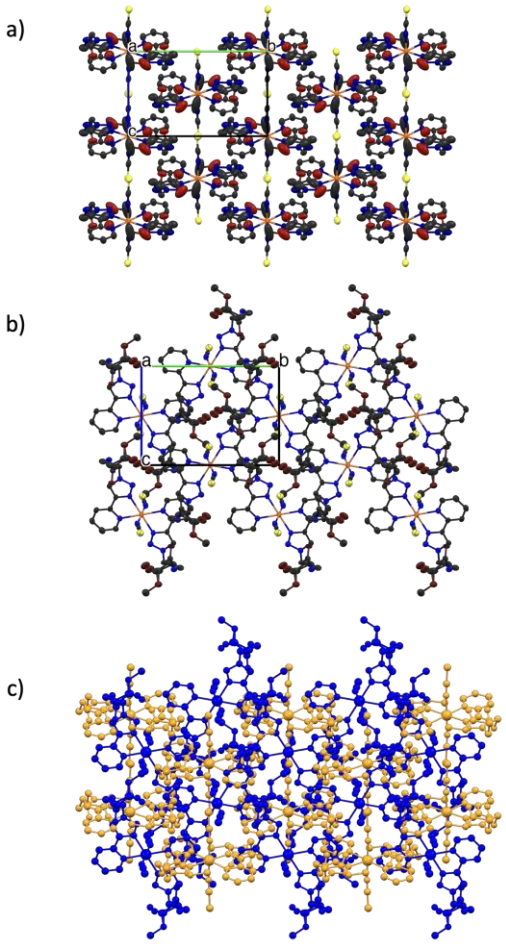

*Figure.5 a) Packing representation of **(1)** at 200 K in the (011) plane, b) Packing representation of **(2)** in the (011) plane, c) overlay of both structures in (011) plane (Orange HS **(1)**, blue **(2)**).*

The short intermolecular interactions are also quite similar in both structures: **(1)** at 110 and 200 K and **(2)** depict the same shortest interaction O1···N6 at ≃ 2.9 Å. No other weak interactions are present in **(1)**, while for **(2)**, an extra intermolecular interaction between O2A···O2A' around 2.94 Å and an intramolecular interaction between N6···O3 at 3.06 Å can be found (Figure.6) (the search limit was 3.10 Å, 90° in order to list only relevant weak interactions). The Fe-Fe distances between the two compounds are also comparable with 8.48 Å and 8.64 Å for **(1)** at 110 K and 200K respectively, and 8.14 Å for **(2)** (Figure.S6). Thus, the analysis of the crystal packing and the weak intermolecular interactions do not evidence any significant differences that could explain the switching behaviors of **(1)** and the fact that **(2)** remains HS.

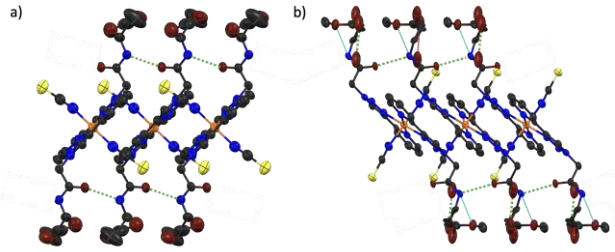

*Figure.6 Inter- (····) and intra- (····) molecular interactions in a) **(1)**-HS and b) **(2)**.*

From the examination of both products, the major distinction between the two compounds resides in the deformation/bending of the Fe-N≡C bond angle of the thiocyanate linker as shown in Figure.6 (172.8°, 170.12° and 160.8° for **(1)** and **(2)** respectively). As already reported, it is known that the thiocyanate ligand binding angle impacts on the SCO properties[27,32]: if the angle varies significantly enough from 180°, the ligand field is decreasing significantly which causes and the compound remains HS. Thus, for compound **(2)**, the ligand deviation of around 20° is likely to be responsible for the crystal field strength decrease, which explains why the compound remains HS at low temperature. Upon inspection of all Fe-N≡C binding of similar compounds (See table.S23),[5-12] compound **(2)** is one of the compounds with the highest angle deviation from 180°, as well as having highly distorted octahedron (large $\boldsymbol{\theta}$ and Σ). More precisely, among the 11 structures reported on 5 different compounds,[5,8,9,10,29] all the compounds which present SCO behavior have an Fe-N≡C angle above 166°. On the opposite, for the only compound ([$Fe^{II}(FTP)_2(NCS)_2$]) that remains in HS state at every temperature, this angle is 145.70°. All of this highly suggest that the ligand field strength is reduced in (**2**), which therefore hinders any thermal SCO properties.

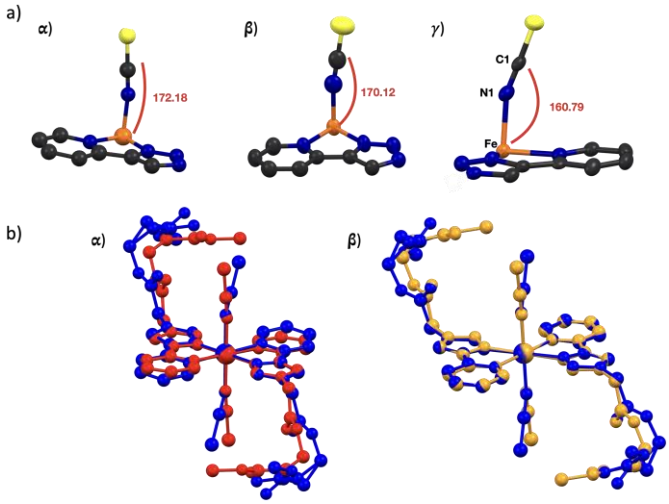

*Figure.7 a) Illustration of the Fe-N-C binding angle in **α) (1)** at 110 K, **β) (1)** at 200 K and **γ) (2)** at 180 K; b) Overlays of **α) (1)** at 110 K and **(2)** at 180 K, **β) (1)** at 200 K and **(2)** at 180 K.*

Additionally, when overlaying both structures, compound (**2**) shows a distinct deformation not only on the octahedron, but also on the functionalized side group which could have a steric impact hindering any movement of the ligand around the iron center. Indeed, the functionalized group is more open (pulled away from the SCN-Fe-NCS axis) in (**1**) compared to (**2**) in both HS and LS states, and the COOMe group is more curled in on itself leading to more constraints around the molecule (Figure.7).

Experimental

Generalities

Metal salts, starting reagent and solvents were purchased from Sigma-Aldrich, Acros Organic and Fisher scientific. Deuterated solvents were purchased from Eurisotop (Cambridge Isotope Laboratories). Distilled water was obtained from MilliQ water, Millipore system.

Powder X-ray Diffraction (PXRD) data were recorded on a high-throughput Bruker D8 Advance diffractometer working on transmission mode and equipped with a focusing Göbel mirror producing CuKα radiation (λ = 1.5418 Å) and a LynxEye detector. (See ESI Figure.S2 and S4)

Single X-ray diffraction. For **(1)**, the data were recorded at 110 K at Synchrotron SOLEIL on the PROXIMA-2 beamline (CCDC 2403577, 2403573). For **(2)**, Single-crystal X-Ray intensity data collection was carried out at 180 K with a four-circle kappa-axis Bruker D8 Venture diffractometer equipped with Mo wavelength X-ray microsource and photon III C14 detector (CCDC 2345551).

Infrared spectra were measured on a Nicolet iS5 FTIR ThermoFisher spectrometer at room temperature, with a resolution of 2 cm^{-1}, averaging 16 scans at 1.0 $cm^{-1}{\cdot}min^{-1}$.

Magnetic susceptibility was recorded with a Quantum Design SQUID magnetometer between 10 and 300 K at a sweep rate of 2 K/min under an applied field of 5 kOe. Samples of ca. 10 mg were enclosed in a diamagnetic sample holder. The data were normalized to get the magnetic susceptibility by mole of iron complex.

NMR ^{1}H and ^{13}C were measured with Bruker 300 Ultrashield spectrometer.

Synthesis

Compound **(1)** was synthesized in thin slow diffusion tubes (length 25 cm, diameter of 5 mm), where 2/3 of the tube was filled with 6 mL of a solution of iron(II) tetrafluoroborate hexahydrate salt (70 mg, 0.21 mmol) with potassium thiocyanate (36 mg, 0.42 mmol) in water. The top layer of the tube was covered with 4 mL of a methanolic solution of PytaCOOMe (97.9 mg, 0.42 mmol). After 7 days, little yellow crystals plate appeared as a polycrystalline powder (Yield: 28%). Elemental Analysis Theoretical: C 44.81%, H 4.03%, N 22.39%, S 8.54%, Found C 44.72%, H 3.97%, N 21.99%, S 8.27%.

Compound **(2)** was synthesized using the same solution/ concentration as compound **(1)**. However, both solutions were mixed at room temperature for 10 minutes before being placed in a large beaker, crystals were recovered in less than 30 minutes as yellow needle like crystals (Yield: 49%). Elemental Analysis Theoretical: C 44.81%, H 4.03%, N 22.39%, S 8.54%, Found C 44.32%, H 3.44%, N 22.27%, S 8.56%.

Conclusions

Two new SCO Fe(II) polymorphic compounds based on a bidentate ligand and two ancillary NCS^- co-ligands have been prepared and structurally characterized. These compounds show quite similar structures through the packing as well as the intermolecular interactions. Even though they are polymorphs, they show two highly different thermal SCO behaviours: compound **(1)** showed a sharp and complete spin crossover with a T ½ = 150 K while compound **(2)** stayed HS down to 10 K. This study highlights that, in this case, the packing is not determinant to rationalize the SCO properties of the compounds, but that the deformation and the angle binding around the FeN_6 octahedron, in particular the Fe-N≡CS bond angle, have a huge impact on the observed switching behaviours. To have in the future a better understanding of this binding and angle dependence properties, new series of compounds having polymorphic equivalent should be studied thoroughly and especially ones with other functional groups.

Author Contributions

E.C. did all the coordination synthesis and wrote the first version of the manuscript. N.D. made the ligand, J.M. recorded the single crystal X-ray for compound **(2)**. All the work was supervised by A.T.

Conflicts of interest

There are no conflicts to declare.

Acknowledgements

A.T. and E.C. thanks the ANR MOFSCO (ANR-18-CE09-0005-01) for funding the project.

Notes and references

1 M.A. Halcrow, *Spin-Crossover Materials: Properties and Applications,* John Wiley & Sons Ltd, 2013, Chapter I-III; P. Gütlich, H.A. Goodwin, Spin Crossover in Transition Metal Compounds I. *Top Curr. Chem*., 2004, 233.

2 H.A. Goodwin, *Coord. Chem. Re*V. 1976, **18**, 293; P. Gütlich, *Struct. Bonding (Berlin),* 1981, **44**, 83; E. König, G. Ritter, S.K. Kulshreshtha, *Chem. Re*V. 1985, **85**, 219; P. Gütlich, A. Hauser, H. Spiering, H. *Angew. Chem., Int. Ed. Engl*. 1994, **33**, 2024; V. Ksenofontov, A.B. Gaspar, J. A. Real, P. Gütlich, *J. Phys. Chem. B*, 2001, **105**, 12266; Y. Qi, E. W. Müller, H. Spiering, P. Gütlich, *Chem. Phys. Lett.* 1983, **101**, 50; A. Bousseksou, F. Varret, M. Goiran, K. Boukheddaden, J. P. Tuchagues, in *Spin Crossover Transit. Met. Compd. III*, Springer Berlin Heidelberg, 2004, **65**; A.Bousseksou, N. Negre, M. Goiran, L. Salmon, J.-P. Tuchagues, M.-L. Boillot, K. Boukheddaden, F. Varret, *Eur. Phys. J. B,* 2000, **13**, 451 ; G. Chastanet, M. Lorenc, R. Bertoni, C. Desplanches, *C. R. Chimie*, 2018, **21**, 1075; F. Renz, H. Spiering, H. A. Goodwin, P. Gütlich, *Hyper. Inter*., 2000, **126**, 155; E. Freysz, S. Montant, J.-F. Létard, *Chem. Phys. Lett.*, 2004, **394**, 318; J. Degert, N.Lascoux, S. Montant, S. Létard, E. Freysz, G. Chastanet, J.-F. Létard, *Chem. Phys. Lett.*, 2005, **415**, 206 ; M. Fumanal, F. Jimenez, J. Ribas-Arino, S. Vela, *Inorg. chem.,* 2017, **56**, 4474.

3 P. Guionneau, M. Marchivie, G. Bravic, J.-F. Létard, D. Chasseau, *Top. Curr. Chem.*, 2004, **234**, 97; M.-L. Boillot, B. Weber, *Comptes Rendus Chimie*, 2018, **21**, 1196; N. Moliner, M. C. Muñoz, P. J. Van Koningsbruggen, J. A. Real, *Inorg. Chim. Acta*, 1998, **274**, 1; K. Madeja, E. König, *Inorg. Nucl. Chem.*, 1963,**25**, 377; M. A. Halcrow, *Chem. Soc. Rev*., 2011, **40**, 4119.

4 H. Phan, J.J. Hrudka, D. Igimbayeva, L.M. Lawson Daku, M.A. Shatruk, *J. Am. Chem. Soc.* 2017, ***139***, 18, 6437.
5 T. Romero-Morcillo, F.J. Valverde-Muñoz, L. Piñeiro-López, M.C. Muñoz, T. Romero, P. Molina, J.A. Real, *Dalton Trans.* 2015, **44**, 43, 18911.
6 J. Conradie, M.M. Conradie, Z. Mtshali, D. van der Westhuizen, K.M. Tawfiq, M.J. Al-Jeboori, S.J. Coles, C. Wilson, J.H. Potgieter, *Inorganica Chimica Acta*, 2019, **484**, 375.
7 M. Ashra Khorasani, N. Wu, O. Fleischel, G. Schatte, A. Petitjean, *Cryst. Growth Des.* 2018, **18**, 3, 1517.
8 V. Niel, A. B. Gaspar, M. C. Muñoz, B. Abarca, R. Ballesteros, J. A. Real, *Inorg. Chem.*, 2003, **42**, 15, 4782.
9 C.-F. Sheu, K. Chen, S.-M. Chen, Y.-S. Wen, G.-H. Lee, J.-M. Chen, J.-F. Lee, B.-M. Cheng, H.-S. Sheu, N. Yasuda, Y. Ozawa, K. Toriumi, Y. Wang, *Chemistry – A European Journal* 2009, **15**, 10, 2384.
10 Z. Arcís-Castillo, L. Piñeiro-López, M. C. Muñoz R. Ballesteros, B. Abarca, J. A. Real, Cryst. Eng. Comm., 2013, **15**, 3455.
11 S.K Vellas, J.E.M. Lewis, M. Shankar, A. Sagatova, J.D.A. Tyndall, B.C. Monk, C.M. Fitchett, L.R. Hanton, J.D. Crowley, *Molecules,* 2013, ***18***, 6383.
12 K.A. Stevenson, C.F.C. Melan, O. Fleischel, R. Wang, A. Petitjean, *Cryst. Growth Des.* 2012, **12**, 11, 5169.
13 C.T. McTernan, T.K. Ronson, J.R. Nitschke, *J. Am. Chem. Soc.* 2019, ***141***, 17, 6837.
14 R.A.S Vasdev, D. Preston, S. Ø. Scottwell, H. J. L. Brooks, J.D. Crowley, M.P. Schramm, *Molecules,* 2016, **21**, 11, 1548.
15 N. Wu, F.C.C. Melan, K. A. Stevenson, O. Fleischel, H. Guo, F. Habib, R.J. Holmberg, M. Murugesu, N.J. Mosey, H. Nierengartene, A. Petitjean. ***Dalton Trans.***, 2015, **44**, 14991.
16 B. Akhuli, L. Cera, B. Jana, S. Saha, C.A. Schalley, P. Ghosh, *Inorg. Chem.* 2015, **54**, 9, 4231.
17 Z. Arcis-Castíllo, S. Zheng, M.A. Siegler, O. Roubeau, S. Bedoui, *Chemistry*, 2011, **17**, 52, 14826; B. Benaicha B, K. Van Do, A. Yangui, N. Pittala, A. Lusson, M. Sy, G. Bouchez, H. Fourati, C.J. Gómez-García, S. Triki, K. Boukheddaden, *Chem Sci.* 2019, **10**, 28, 6791; J. G. Haasnoot, G. Vos, W.L. Groeneveld, *Z. Naturforsh. B.,* 1977, **32**, 1421; O. Kahn, J. Krober, C. Jay, *Adv. Mater.*, 1992, **4**, 718; J. J. A. Kolnaar, M. I. de Heer, H. Kooijman, A. L. Spek, G. Schmitt, V. Ksenofontov, P. Gütlich, J. G. Haasnoot, J. Reedijk, *Eur. J. Inorg. Chem.*, 1999, **5**, 881; A. Sugahara, H. Kamebuchi, A. Okazawa, M. Enomoto, N. Kojima, *Inorganics*, 2017, **5**, 3, 50; F.-L. Liu, D. Li, L.-J. Su, J. Tao, *Dalton Trans.*, **2018**, 47(5), 1407; H. O. Bayer, R. S. Cook, W. C. von Mayer, *US Pat*. 1974, 3,821,376; T. Yokoyama, Y. Murakami, M. Kiguchi, T. Komatsu, N. Kojima, *Phys. Rev.B*, 1998, **58**, 14238.
18 G. Schanne, L. Henry, H.C. Ong, A. Somogyi, K. Medjoubi, N. Delsuc, C. Policar, F. Garcia, H. C. Bertrand, ***Inorg. Chem. Front.***, 2021, **8**, 3905.
19 S. Hostachy, M. Masuda, T. Miki, I. Hamachi, S. Sagan, O. Lequin, K. Mejoubi, A. Somogyi, N. Delsuc, C. Policar, ***Chem. Sci.,*** 2018, **9**, 4483.
20 H.Y.V. Ching, X. Wang, M. He, N. Perujo Holland, R. Guillot, C. Slim, S. Grivau, H. C. Bertrand, C. Policar, F. Bedioui, M. Fontecave, *Inorg. Chem.*, 2017, **56**, 5, 2966.
21 S. Clède, C. Policar, *Chem. Eur. J.,* 2015, **21**, 942.
22 E. Koenig, K. Madeja, K.J. Watson, *J. Am. Chem. Soc.* 1968, **90**, 5, 1146.
23 B. Moulton, M. J. Zaworotko, *Chem. Rev.*, 2001, **101**, 6, A629.
24 T. M. Ross, B. Moubaraki, S. M. Neville, S. R. Batten, K. S. Murray, *Dalton trans.*, 2012, **21**, 1512.
25 E. Tailleur, M. Marchivie, P. Negrier, D. Denux, S. Massip, D. Mondieig, G. Chastanet, P. Guionneau, *CrystEngComm*., 2019, **21**, 6246.
26 Y.-X Huang, H.-J. Hu, R.-J. Wei, G.-H. Ning, D. Li, *Cryst. Growth Des.* 2021, **18**, 3, 4587
27 E. Cuza, C. D. Mekuimemba, N. Cosquer, F. Conan, S. Pillet, G. Chastanet, S. Triki, *Inorg. Chem.*, 2021, **60**, 9, 6536.
28 J. Tao, R.-J. Wei, R.-B. Huang, L.-S. Zheng, *Chem. Soc. Rev.,* 2012, **41**, 703.
29 H.S. Scott, C. J. Gartshore, S.-X. Guo, B. Moubaraki, A.M. Bond, S.R. Batten, K.S. Murray, ***Dalton Trans.***, 2014, **43**, 15212.
30 S. Hostachy, J.-M. Swiecicki, C. Sandt, N. Delsuc, C. Policar, *Dalton Trans.,* 2016, **45**, 2791.
31 P. Guionneau, M. Marchivie, G. Bravic, J.-F. Létard, D. Chasseau, *J. Mater. Chem.*, 2002, **12**, 2546; J. K. McCusker, A. L. Rheingold, D. N. Hendrickson, *Inorg. Chem*., 1996, **35**, 2100; P. Guionneau, C. Brigouleix, Y. Barrans, A. E. Goeta, J.-F. Létard, J. A. Howard, J. Gaultier, D. Chasseau, *C. R. Acad. Sci. Ser. IIc*, 2001, **4**, 161; F. A. Deeney, C. J. Harding, V. McKee, G. G. Morgan; J. Nelson, S. J. Teat, W. Clegg, *Dalton Trans*., 1998, 1837; M. G. B. Drew, C. J. Harding, V. McKee, G. G. Morgan, J. Nelson, *J. Chem. Soc. Chem. Comm*., 1995, 1035; M. Marchivie, P. Guionneau, J. F. Létard, D. Chasseau, *Acta Crystallogr. Sect. B Struct. Sci*., 2005, **61**, 25.
32 S. Rodríguez-Jiménez, S. Brooker, Inorg. Chem. 2017, 56, **22**, 13697.